http://ansinet.com/itj

ITJ

ISSN 1812-5638

INFORMATION TECHNOLOGY JOURNAL

ANSInet
Asian Network for Scientific Information
308 Lasani Town, Sargodha Road, Faisalabad - Pakistan

Information Technology Journal 12 (24): 8102-8108, 2013
ISSN 1812-5638 / DOI: 10.3923/itj.2013.8102.8108

Research on Nonlinear Vibration Characteristics of Non-orthogonal Face Gear Transmission

[2]Huang Long, [1,2]Yu Guang-Bin, [2]Chen Ju-Hui, [1]Zhao Yang and [2]Zhao Lei
[1]Harbin Institute of Technology, Harbin, Heilongjiang, 150001, China
[2]School of Mechanical and Power Engineering, Harbin University of Science and Technology, Harbin, Heilongjiang, 150080, China

Abstract: Based on the concentrated parameters theory, a 7-freedom coupled vibration dynamic model of the non-orthogonal face gear transmission system is established, which includes time-varying mesh stiffness, the tooth backlash clearance and transmission error. In the model, the torsion oscillation of the gear pair, the axial vibration aroused by tooth meshing force and the lateral oscillations resulting from flexional deformation of the gear shaft are taken into account. The mesh stiffness fluctuation is developed as 5-order Fourier series and the tooth backlash clearance is fitted by 7-order polynomial function. Through the Gear method, the dynamic response of the system is obtained and the vibration characteristics are analyzed.

Key words: Non-orthogonal face gear, time-varying mesh stiffness, tooth backlash, nonlinear vibration

INTRODUCTION

Face gear transmission is a form of gear transmission, which is similar to the situation where a cylindrical gear meshes with a bevel gear (Litvin *et al*., 1992). Compared with the bevel gear transmission, face gear transmission has such outstanding advantages as smaller size, lighter weight, larger transmission ratio and weaker noise and vibration (Litvin *et al*., 1998), thus, extensive and in-depth studies have been made by foreign and domestic scholars (Grendal, 1996; Litvin *et al*., 2000; Zhu and Gao, 1999; Yang *et al*., 2010; Lin and Ran, 2012). However, domestic studies are rather rare (Wang *et al*., 2009) and mainly concentrated on orthogonal cases. So, it is both necessary and meaningful to do research on nonlinear vibration characteristics of non-orthogonal face gear transmission system.

In this study, the nonlinear dynamics model including the tooth backlash, time-varying mesh stiffness and error for the non-orthogonal face gear transmission system is established. Besides, the numerical calculation and analysis of the nonlinear vibration characteristics of the system response are obtained (Yu *et al*., 2007).

VIBRATION MODEL OF NON-ORTHOGONAL FACE GEAR TRANSMISSION

Based on the theory of concentrated parameters, the dynamic model of the non-orthogonal face gear transmission system is established, which is shown in Fig. 1, where gear 1 is the cylindrical gear 1 and 2 is the non-orthogonal face gear. $O\text{-}x_1y_1z_1$ and $O\text{-}x_2y_2z_2$ are, respectively the coordinate system fixed on gear 1 and 2. The intersecting angle of the center axes of the two gears $<x_1oz_2 = \delta$. There are totally seven vibrational degrees of freedom of the dynamic model of the system. X_i, Y_i and z_i are, respectively the translational degrees of freedom of the gear $_i$; ϕ_i is the rotational degrees of freedom of the gear i(i = 1, 2).

VIBRATION DIFFERENTIAL EQUATIONS OF THE SYSTEM

Force analysis of the gear teeth: The dynamic normal load of the gear pair is F_n, which can be decomposed into three component forces: F_{iy}, F_{iz} and F_{ix} (i = 1, 2):

$$\begin{cases} F_n = k(t)\cdot f(\Lambda)+c_m\cdot\dot{\Lambda} \\ F_{1y} = F_n\cdot\cos\alpha_n \\ F_{1z} = F_n\cdot\sin\alpha_n \\ F_{2y} = F_n\cdot\cos\alpha_n \\ F_{2z} = F_n\cdot\sin\alpha_n\cdot\cos(90°\text{-}\delta) \\ F_{2x} = F_n\cdot\sin\alpha_n\cdot\sin(90°\text{-}\delta) \end{cases} \quad (1)$$

where, k(t) is the normal time-varying mesh stiffness of the gear teeth; c_m is the normal damping of the gear teeth meshing; $f(\Lambda)$ is the nonlinear function of the meshing gear pair.

Corresponding Author: Yu Guang-Bin, School of Mechanical and Power Engineering, Harbin University of Science and Technology, Harbin, Heilongjiang, 150080, China

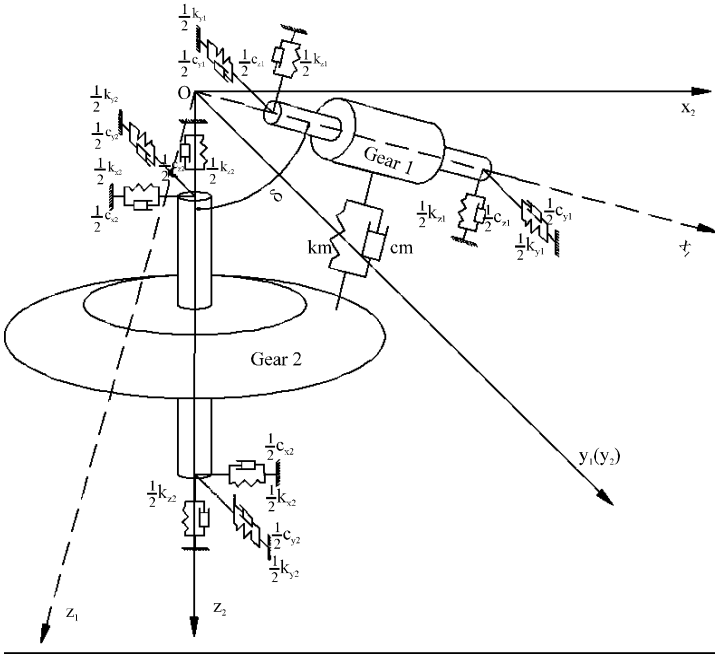

Fig. 1: Dynamic model of non-orthogonal face gear transmission

Time-varying mesh stiffness: The gear teeth meshing composite stiffness would periodically vary with the alternate happening of the single and double meshing tooth pairs, thus it can be developed into high order Fourier series:

$$k(t) = k_m + \sum_{1=1}^{5} A_{kl} \cdot \cos(1 \cdot \Omega_h \cdot t + \theta_{kl}) \quad (2)$$

where, k_m is the average value of the time-varying mesh stiffness; A_{kl} is the /-order harmonic amplitude; θ_{kl} is the /-order initial phase.

Non-linear description of the tooth backlash: The non-analytic function $f(\Lambda)$ is introduced to describe the actual deformation of the gear teeth with consideration of the backlash:

$$f(\Lambda) = \begin{cases} \Lambda - b, \Lambda > b \\ 0, -b \le \Lambda \le b \\ \Lambda + b, \Lambda < -b \end{cases} \quad (3)$$

where, symbol b is the half of the normal mean backlash. The image of the function $f(\Lambda)$ is shown in Fig. 2.

Normal relative displacement of the meshing point: Under the meshing force, the normal relative displacement of the meshing point Λ is expressed as follows:

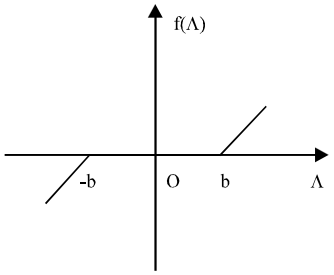

Fig. 2: Function image of $f(\Lambda)$

$$\Lambda = \Lambda_n + \Lambda_\phi - e_n(t) \quad (4)$$

where, Λ_n and Λ_ϕ are, respectively the normal relative translational and rotational displacement of the meshing point, $e_n(t)$ is the statistic normal transmission error of the gear pair:

$$\Lambda_n = Z_1 \cdot \sin\alpha_n + Y_1 \cdot \cos\alpha_n - [Z_2 \cdot \cos(90° - \delta) \cdot \sin\alpha_n + Y_2 \cdot \cos\alpha_n + X_2 \cdot \sin(90° - \delta) \cdot \sin\alpha_n] \quad (5)$$

$$\Lambda_\phi = (r_1, \phi_1 - r_2.\phi_2). \cos\alpha_n \quad (6)$$

where, r_1 is the distance between the meshing point of the tooth surface and the center axis of gear$_i$; α_n is the pressure angle of the normal plane:

$$e_n(t) = \sum_{1=1}^{N_s} A_{el} \cdot \cos(1 \cdot \Omega_h \cdot t + \theta_{el}) \quad (7)$$

where, A_{el} is the /-order harmonic amplitude of the error; Ω_h is the angular frequency of the gear pair; θ_{el} is the /-order initial phase of the statistic transmission error. From above all, Λ can be expressed as follows:

$$\begin{aligned}\Lambda &= (Y_1-Y_2)\cdot\cos\alpha_n+[Z_1-Z_2\cdot\cos(90°-\delta)]\cdot\sin\alpha_n\\ &-X_2\cdot\sin(90°-\delta)\cdot\sin\alpha_n+(r_1\cdot\phi_1-r_2\cdot\phi_2)\cdot\cos\alpha_n\\ &-\sum_{1=1}^{N_e}A_{el}\cdot\cos(l\cdot\Omega_h\cdot t+\theta_{el})\end{aligned} \tag{8}$$

Vibration differential equations of the system: Based on all above, vibration differential equations of the system can be written as follows, which are the 7-freedom, positive semi-definite, varying-parameter and 2-order non-linear differential equations:

$$\begin{cases}M_1\cdot\ddot{Y}_1+c_{y1}\cdot\dot{Y}_1+k_{y1}\cdot Y_1=-F_{1y}\\ M_1\cdot\ddot{Z}_1+c_{z1}\cdot\dot{Z}_1+k_{z1}\cdot Z_1=-F_{1z}\\ I_{1x}\cdot\ddot{\phi}_1=T_1-F_n\cdot r_1\\ M_2\cdot\ddot{Y}_2+c_{y2}\cdot\dot{Y}_2+k_{y2}\cdot Y_2=F_{2y}\\ M_2\cdot\ddot{Z}_2+c_{z2}\cdot\dot{Z}_2+k_{z2}\cdot Z_2=F_{2z}\\ M_2\cdot\ddot{X}_2+c_{x2}\cdot\dot{X}_2+k_{x2}\cdot X_2=F_{2x}\\ I_{2z}\cdot\ddot{\phi}_2=-T_2+F_n\cdot r_2\end{cases} \tag{9}$$

where, M_j is lumped mass of the gear $_i$; I_{ix} is moment of inertia of gear $_i$; k_{ij} and c_{ij} (i = 1, 2, j = y, z, x) are separately brace stiffness and damping along the direction of the x_i-axis y_i-axis and Z_i-axis. T_I is the torque acting on gear i (i = 1, 2):

$$\begin{aligned}T_1&=F_{1m}\cdot r_1+\frac{F_{1v}\cdot I_{1x}}{M_e\cdot r_1}\\ T_2&=F_{2m}\cdot r_2=F_{1m}\cdot r_2\end{aligned} \tag{10}$$

where, F_{1m} and F_{iv} are separately the constant part and variation part of the peripheral force which the gear 1 bears, M_e is the equivalent mass of the gear pair:

$$M_e=\frac{I_{1x}\cdot I_{2z}}{I_{1x}\cdot r_2^2+I_{2z}\cdot r_1^2} \tag{11}$$

By the introduction of a new variable Λ, ϕ_1 and ϕ_2 can be eliminated, so the degrees of freedom of the system are reduced from seven to six. Then Eq. 9 can be transformed into dimensionless differential equations:

$$\begin{cases}\ddot{y}_1(\tau)+2\zeta_{y1}\cdot\dot{y}_1(\tau)+2p_2\cdot\zeta_{m1}\cdot\dot{\lambda}(\tau)\\ +\kappa_{y1}\cdot y_1(\tau)+p_2\cdot\kappa_{m1}\cdot g[\lambda(\tau)]=0\\ \ddot{z}_1(\tau)+2\zeta_{z1}\cdot\dot{z}_1(\tau)+2p_1\cdot\zeta_{m1}\cdot\dot{\lambda}(\tau)\\ +\kappa_{z1}\cdot z_1(\tau)+p_1\cdot\kappa_{m1}\cdot g[\lambda(\tau)]=0\\ \ddot{y}_2(\tau)+2\zeta_{y2}\cdot\dot{y}_2(\tau)-2p_2\cdot\zeta_{m2}\cdot\dot{\lambda}(\tau)\\ +\kappa_{y2}\cdot y_2(\tau)-p_2\cdot\kappa_{m2}\cdot g[\lambda(\tau)]=0\\ \ddot{z}_2(\tau)+2\zeta_{z2}\cdot\dot{z}_2(\tau)-2p_1\cdot p_4\cdot\zeta_{m2}\cdot\dot{\lambda}(\tau)\\ +\kappa_{z2}\cdot z_2(\tau)-p_1\cdot p_4\cdot\kappa_{m2}\cdot g[\lambda(\tau)]=0\\ \ddot{x}_2(\tau)+2\zeta_{x2}\cdot\dot{x}_2(\tau)-2p_1\cdot p_3\cdot\zeta_{m2}\cdot\dot{\lambda}(\tau)\\ +\kappa_{x2}\cdot x_2(\tau)-p_1\cdot p_3\cdot\kappa_{m2}\cdot g[\lambda(\tau)]=0\\ \ddot{\lambda}(\tau)+2p_2\cdot\zeta_m\cdot\dot{\lambda}(\tau)+p_2\cdot\kappa(\tau)\cdot g[\lambda(\tau)]\\ +p_1\cdot p_3\cdot\ddot{x}_2(\tau)-p_2\cdot\ddot{y}_1(\tau)\\ +p_2\cdot\ddot{y}_2(\tau)-p_1\cdot\ddot{z}_1(\tau)+p_1\cdot p_4\cdot\ddot{z}_2(\tau)\\ -f_{1m}-f_{1v}+f_e=0\end{cases} \tag{12}$$

SOLUTION AND ANALYSIS FOR VIBRATION DIFFERENTIAL EQUATIONS

The Gear method is one of the most effective general solutions for complex non-linear differential equations. The main advantages of the Gear method are the automatically changed step-size and orders, as well as fast calculation speed which contributes to the solution of large-scale differential equations. By use of the Gear method, the Eq. 12 can be smoothly solved to obtain the response of the system. The calculation is conducted under the assumption that the driving-torque and load-torque are both stable. With the changes of meshing frequency, the vibration characteristics of system response also shows a different variation.

Figure 3 shows when excitation frequency $\omega_h = 1.03$, the system response is single period non-harmonic response, which is similar to the characteristics of linear system, i.e,. single-frequency excitation and single-frequency response. The time response courses of the relative normal vibration displacement are simple harmonic waves. The phase plane plot is a certain closed curve which is neither a circle nor an elliptic curve. The Poincare map is a single discrete point.

Figure 4 shows the 2-period sub-harmonic response of the system when $\omega_h = 1.22$, which reflects a periodic motion whose period is 2T. The corresponding phase plane plot is some kind of closed non-circle curve. The Poincare map is two discrete points. The distribution of the spectral lines is shown at the discrete points in the form of m. $\omega_h/2$ in FFT spectrogram.

Figure 5 shows the quasi-periodic response of the system when $\omega_h = 1.95$. The response is an approximate periodic motion, which is a combination of two or more periodic motions, with no minimal period. The corresponding phase plane plot is many curve circles which are filled with a certain region. The Poincare map is a rapture ring made up of several discrete points. The spectral lines in FFT spectrogram are still discretely distributed at the points in the form of frequency combination.

Figure 6 shows that the system response develops into the chaotic response from the quasi-periodic when

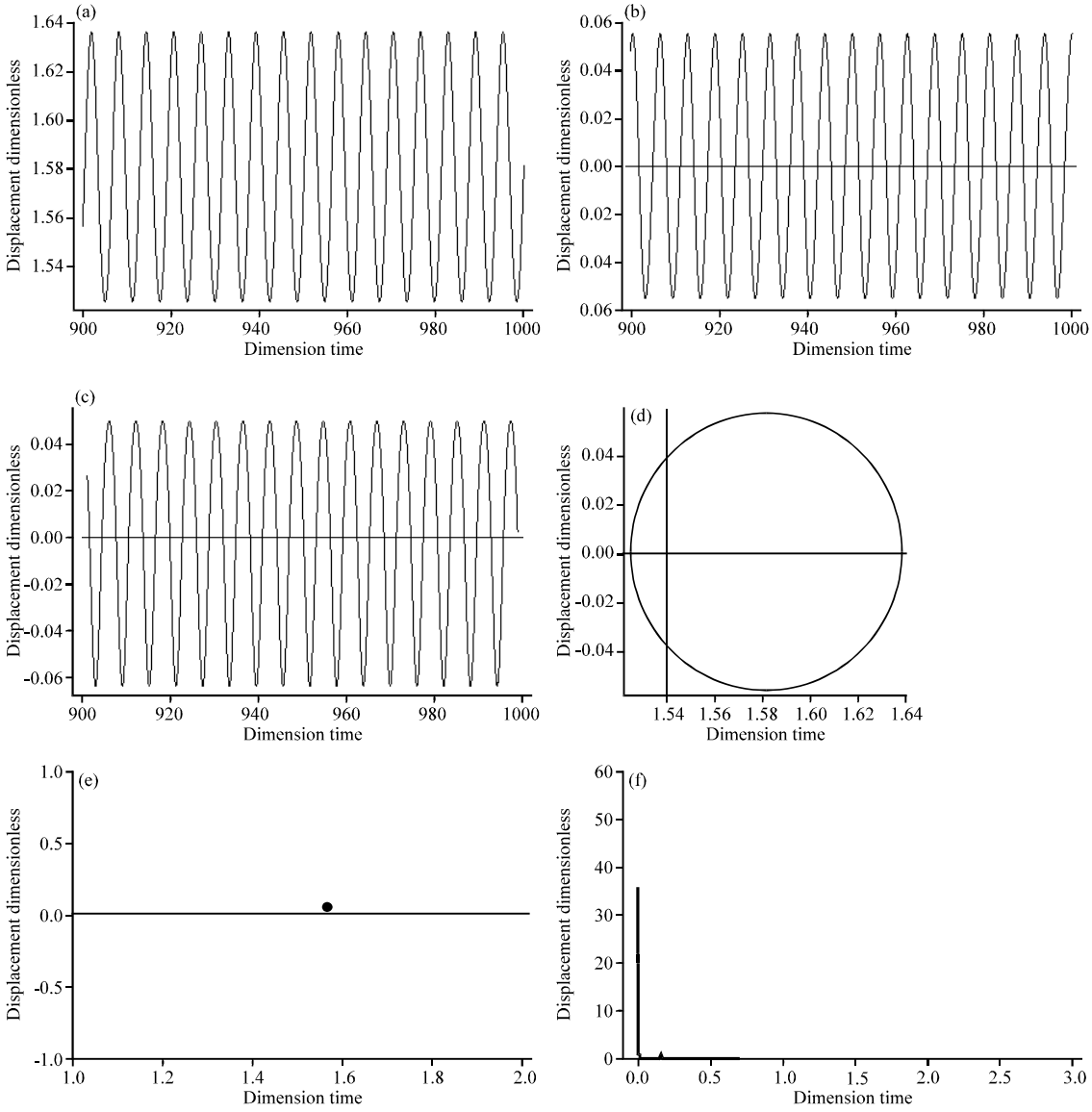

Fig. 3(a-f): System response when ω_n = 1.03, (a-c) Relation of λ and τ, $\dot{\lambda}$ and τ, $\ddot{\lambda}$ and τ, (d) Phase plane, (e) Poincare map and (f) FFT spectrogram

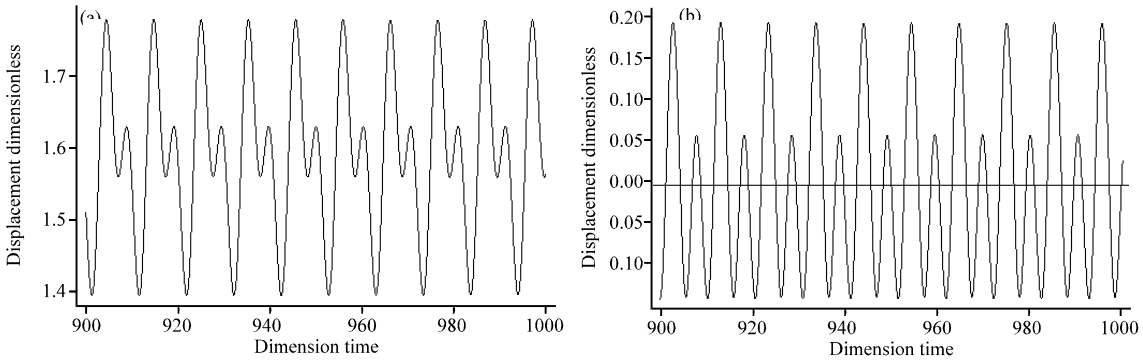

Fig. 4(a-f): Continue

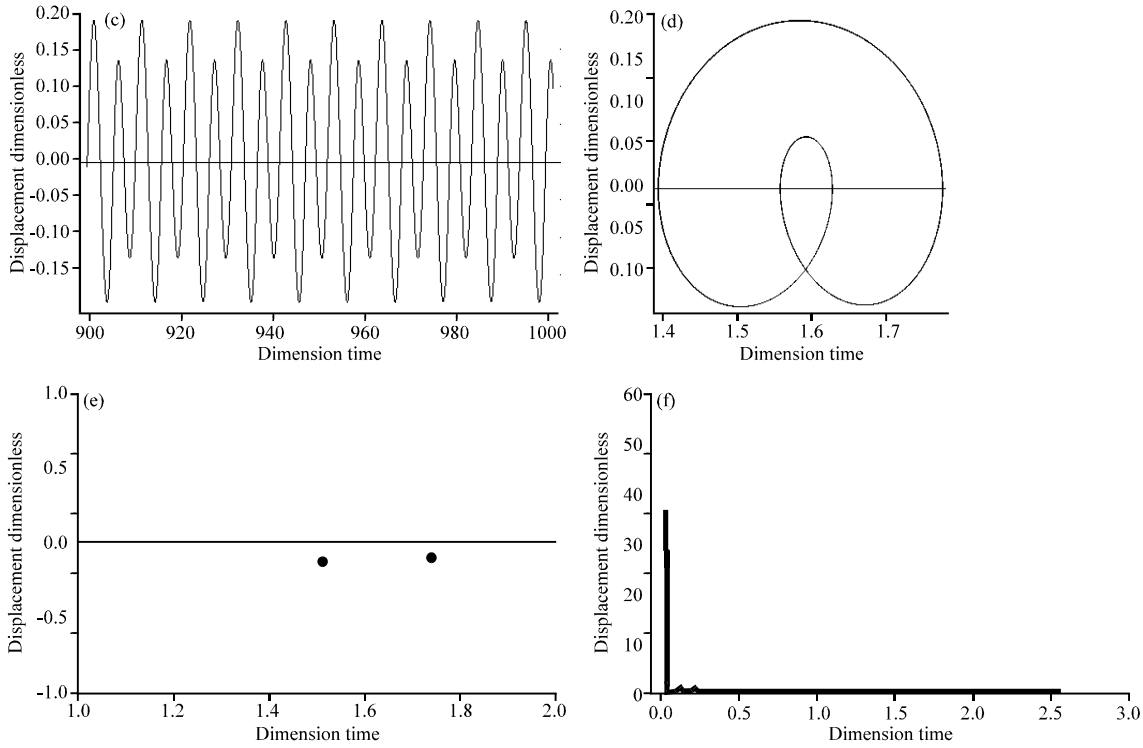

Fig. 4(a-f): System response when $\omega_h = 1.22$, (a-c) Relation of λ and τ, $\dot{\lambda}$ and τ, $\ddot{\lambda}$ and τ, (d) Phase plane, (e) Poincare map and (f) FFT spectrogram

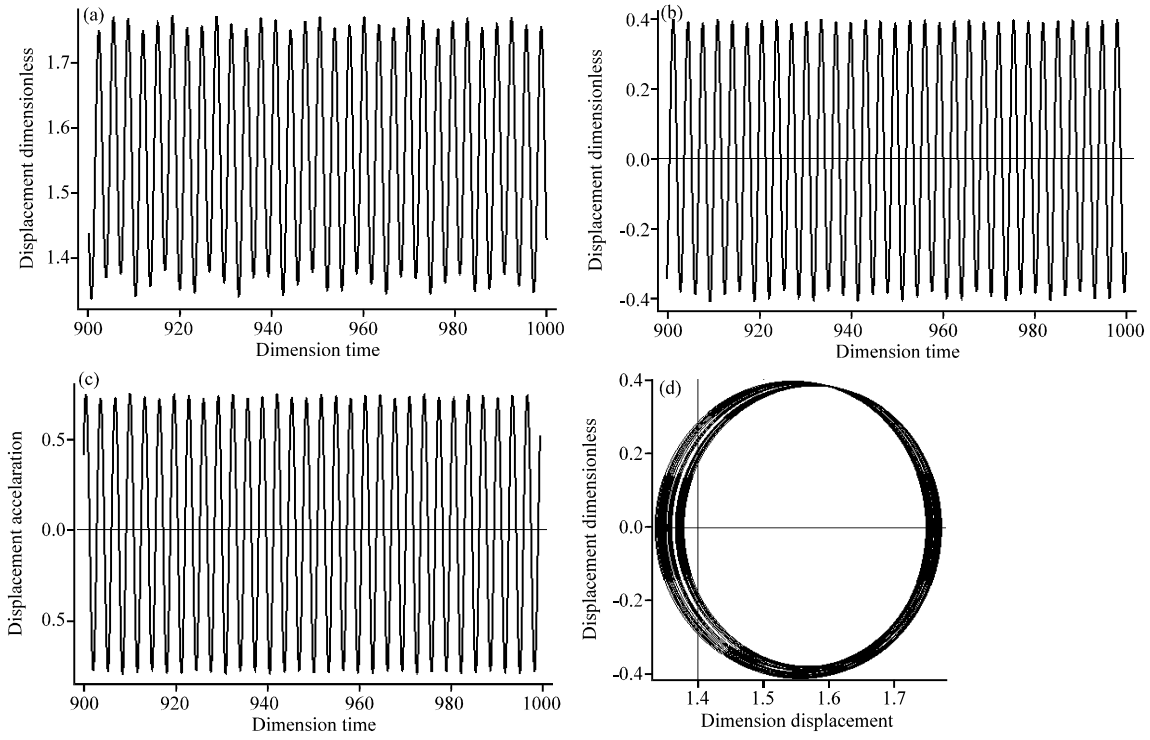

Fig. 5(a-f): Continue

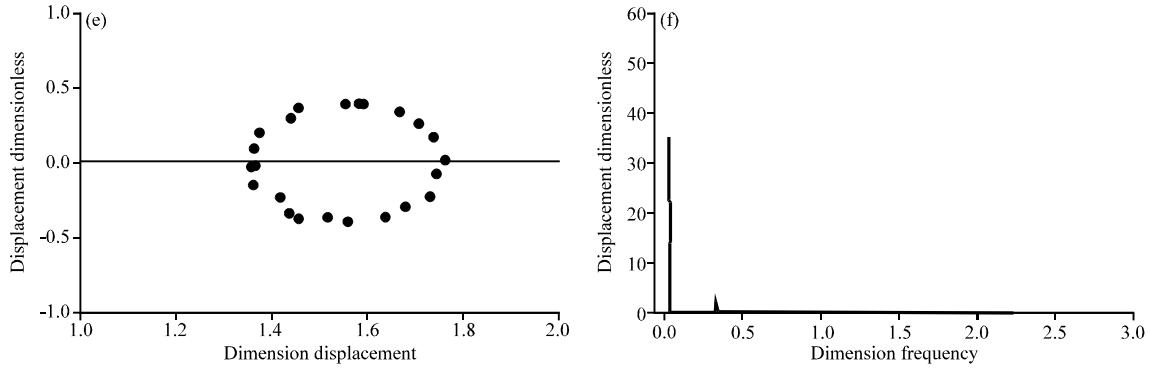

Fig. 5(a-f): System response when ω_h= 1.95, (a-c) Relation of λ and τ, $\dot{\lambda}$ and τ, $\ddot{\lambda}$ and τ, (d) Phase plane, (e) Poincare map and (f) FFT spectrogram

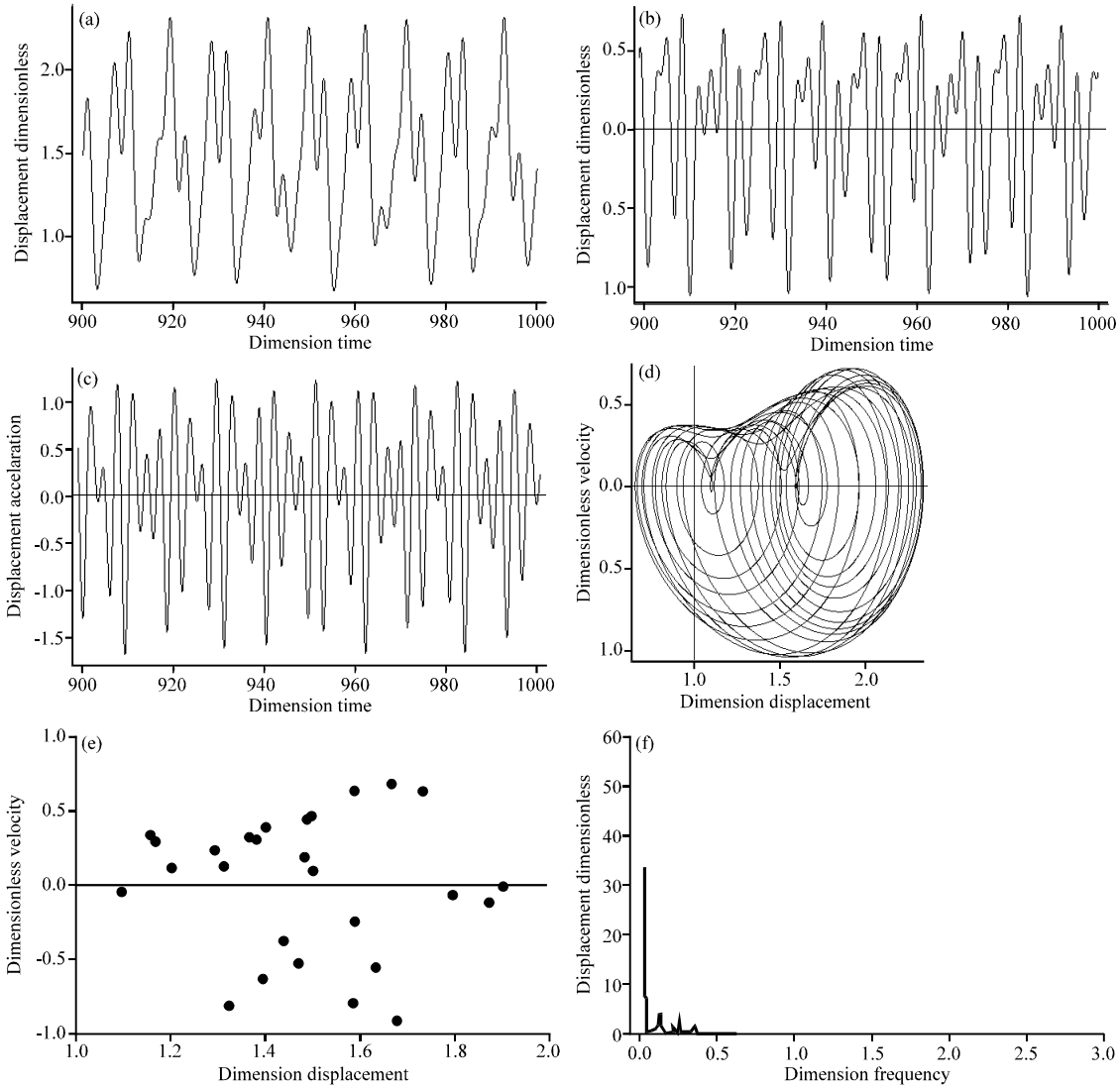

Fig. 6(a-f): System response when ω_h = 2.05, (a-c)Relation of λ and τ, $\dot{\lambda}$ and τ, $\ddot{\lambda}$ and τ, (d) Phase plane, (e) Poincare map and (f) FFT spectrogram

ω_h = 2.05. The response is a non-period response motion with no minimal period. The corresponding phase plane plot consists of many intertwining and intercross but misalignment and not-closed curves. The Poincare map is a set of points which are spread in certain region. The spectral lines in FFT spectrogram are still discretely distributed at the points in the form of frequency combination.

CONCLUSION

The comprehensive analysis of the system dynamic response, including the time response courses, Poincare map, phase plane plots and FFT frequency spectrogram, shows that with the changes of the excitation frequency, a variety of steady-state response of system appears, i.e., single-period non-harmonic response, double-period sub-harmonic response, quasi-periodic response and chaotic response. These characteristics can have a great impact on the gear tooth contact stability and operational reliability of the system. Therefore, when in design, the values of the relevant parameters should be paid attention to, in case that the transmission system being in the chaotic response state.

ACKNOWLEDGMENT

This research was supported by the Harbin City Key Technologies R and D Program under Grant No. 2011AA1BG059 and Key Program of National Natural Science Foundation of Heilongjiang No. ZD201309.

REFERENCES

Grendal, H., 1996. Cylko gears: An alternative in mechanical power transmission. J. Gear Technol., 13: 26-31.

Lin, T.J. and X.T. Ran, 2012. Nonlinear vibration characteristic analysis of a face-gear drive. J. Vibr. Shock, 31: 25-31.

Litvin, F., A. Egelja, J. Tan and G. Heath, 1998. Computerized design, generation and simulation of meshing of orthogonal offset face-gear drive with a spur involute pinion with localized bearing contact. Mech. Mach. Theory, 33: 87-102.

Litvin, F., G. Argentieri, M. De Donno and M. Hawkins, 2000. Computerized design, generation and simulation of meshing and contact of face worm-gear drives. Comput. Methods Applied Mech. Eng., 189: 785-801.

Litvin, F., R.B. Bossler, Y.J.D. Chen, Y. Zhang and J.C. Wang, 1992. Design and geometry of face-gear drives. ASME J. Mech. Des., 114: 642-647.

Wang, H.X., Y. Hou and R.P. Zhu, 2009. Tooth surface equations of non-orthogonal face gear and simulation. Jiangsu Mach. Build. Autom., 38: 94-97.

Yang, Z., S.M. Wang, Y.S. Fan and H.X. Liu, 2010. Nonlinear dynamics of face-gear transmission system. J. Vibr. Shock, 29: 26-35.

Yu, G.B., J.M. Wen, G.X. Li and X. Cao, 2007. Gear method for solving dynamics differential equations of gear systems. Chin. J. Scient. Instrum., 4: 598-600.

Zhu, R.P. and D.P. Gao, 1999. Study on the method of avoiding dedendum undercutting and addendum pointing in face gear design. China Mech. Eng., 11: 1274-1276.